On the Influence of Measurement Setups on Gridded Ion Thruster Plume Potentials

IEPC-2024-1062

Presented at the 38th International Electric Propulsion Conference, Toulouse, France
June 23-28, 2024

Maximilian Maigler*, Ruslan Kozakov†, and Jochen Schein‡
Bundeswehr University, Werner-Heisenberg-Weg 39, 85579 Neubiberg, Germany

Within the framework of test setups for gridded ion thrusters (RITs), diagnostics of the plume are vital for evaluating the thruster's performance. The most important parameters are the distribution of ion and electron velocities, number densities and the plume plasma potential. In a recently carried out test campaign of a mN-class RIT, emissive and Langmuir probes were used to evaluate the plume plasma properties. As also observed for other thrusters such as Hall thrusters, probe measurements of ion beam plumes are found to exert a significant disturbance on the self-neutralization process of the beam, leading to increased plume potentials and different plasma number density compared to non-disturbed ion beams.

Nomenclature

Δt	= discrete time step
Δx	= discrete cell size
u_x	= axial velocity component
d_{ref}	= (variable) hard sphere diameter
m	= mass
n	= number density
i	= subscript: species i
I	= current
E	= energy
e	= elementary charge
e^-	= electron species
j	= current density
$Z+$	= ion species
d_{ij}	= center-center distance
Kn	= Knudsen number
λ	= mean-free path
L	= characteristic length
σ	= collision cross-section
$\mathbf{B}$	= magnetic vector field
$\mathbf{E}$	= electric vector field
T	= temperature
P	= probability
ϕ	= electric potential
U	= voltage
Q	= charge
$\mathbf{T}$	= thrust
$\mathbf{F}$	= force
$\dot{m}$	= mass flow
A	= area

*PhD Student, Institute of Physics, maximilian.maigler@unibw.de
†Research Associate, Institute of Physics, ruslan.kozakov@unibw.de
‡Department Lead, Institute of Physics, js@unibw.de

I. Introduction

Developing electric satellite propulsion systems (EPs) requires extensive experimental testing for evaluation of performance and lifetime of a thruster. Performance assessment is usually carried out using invasive measurement probes that are capable of measuring plasma properties such as the beam current or plasma potential, since the number density of the plasma species, i.e. n_{Z+} and n_{e^-}, are in regimes (1×10^{13} to $1 \times 10^{16}\,\mathrm{m}^{-3}$) that make non-invasive measurements a difficult undertaking.

The objective of this study is to demonstrate that the presence of invasive probes within the plume of EPs, specifically RITs, has a significant impact on the plasma potential in the downstream region of the thruster, potentially falsifying some important experimental results such as the erosion rate on a thruster's exhaust components. Further, the spatial measurement device position relative to the exhaust plume is shown to govern the intensity of how much the self-neutralizing process of an uncompensated ion beam is disturbed. It is common practice to operate small RITs in the µN thrust regime without a neutralizer in vacuum testing facilities, relying entirely on the self-neutralizing phenomenon elicited by secondary electron emission (SEE) through the ion beam interaction with the facility walls, as a neutralizer would introduce too much neutral gas in the vicinity of the thuster.

Diagnostics of invasive plasma probes for EPs are described in detail by Lobbia *et al.*[1] and Sheenan *et al.*[2] The importance of probes being in direct (electrical) contact with the plasma for determining the plasma potential ϕ is discussed in Refs.[3–5] Riege *et al.*[6] elucidated on the effects of ion beams *blowing up* in uncompensated conditions[a].

One of the key quantities influencing erosion rates on thruster components affected by the exhaust plume is the plasma potential. For instance, *pit* and *groove* erosion occurring on the decel grid is mainly governed by the impact energy and flux of bombarding ions coming from the exhaust plume. The higher the difference of potential between the decel grid and exhaust plume, the more acceleration the impacting ion will experience. Additionally, a higher exhaust potential will result in the ion beam slowing down, increasing the probability of charge-exchange (CEX) events and yields higher production rates of slow CEX ions, which account for most of the erosion of the decel grid.[7]

In this study, proving the self-neutralization disturbance and beam potential blow-up through presence of invasive probes was achieved by carrying out Langmuir and emissive probe testing of a µN RIT as well as by means of numerical modeling, obtaining good agreement with results determined in the experiments.

II. Methodology

A. Experimental testing

The experiments were carried out in the in-house vacuum testing facility *R2D2*. The total volume is $4.5\,\mathrm{m}^3$ and includes various pumps (turbomolecular, cryogenic, and rotary vane type) to establish vacuum conditions of $1 \times 10^{-5}\,\mathrm{Pa}$ before, and 1×10^{-4} to $3 \times 10^{-4}\,\mathrm{Pa}$ during thruster operation. The probes were mounted on two units that allow translational movement in one direction, i.e., one in the $x-$ and one in the $y-$direction and measuring steps of 10 mm in each spatial direction were performed. A schematic of the thruster and diagnostic setup is shown in Fig. 1, highlighting the two Langmuir (probes 1 and 3) and two emissive probes (probes 2 and 4).

Probe 1 determines the distance of the measurement apparatus from the thruster's exit plane $x = 0$ and was the total range of $\Delta x = 5$ to 100 mm, while the total range of $\Delta y = -50$ to 50 mm. The thruster is described in detail by Feili *et al.*[8] and was used as the ion source. The calibration and setup of probe diagnostics is outlined in the publication of Kozakov *et al.*[9] As demonstrated there, the effects of disturbance should not only be apparent at the probes themselves, but clearly visible also at the secondary-star-ground (SSG) as well as at the currents measured at the first (screen) and secondary (accel) grids of the thruster.

B. Numerical modeling

The general simulation setup was split into two coherent parts. The first simulation was used to model the flow of only the neutral gas, since the differences in number density between the plasma and the propellant

[a] *Uncompensated conditions* are defined as a scenario where the positive space charge produced by an ion beam is not neutralized by lack of electrons. A local positive potential is formed leading to radial repulsion of an ion beam downstream of the stream direction

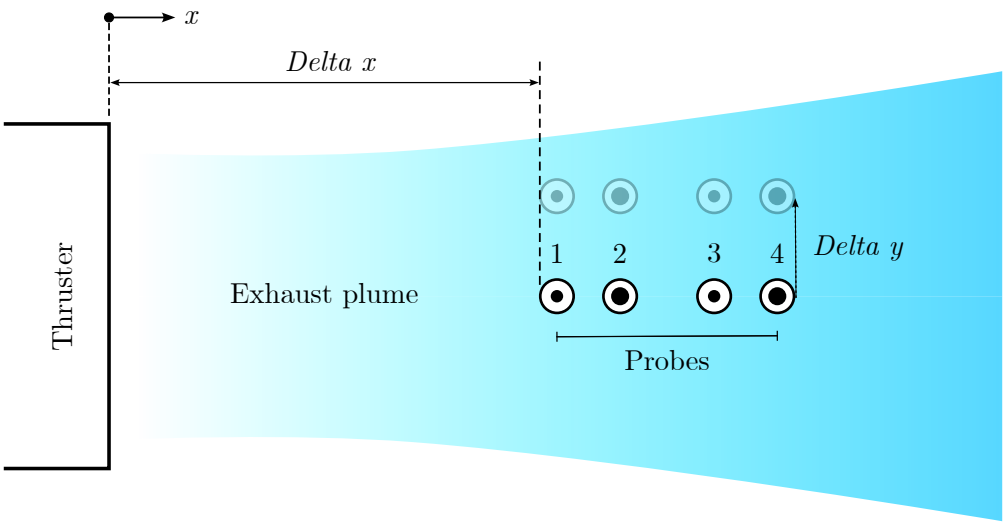

Figure 1. Schematic of experimental setup. µN-RIT on the left side and probes located inside the ion beam with axial (Δx) and radial (Δy) shifting throughout the centerline plane. The apparatus serves for measuring the plasma potential, electron number density and temperature, respectively.

are of at least one magnitude in the exhaust plume, making direct collision modeling between these species negligible. The results for this first simulation were then time-averaged to obtain a mean spatial distribution of the neutral gas number density, temperature, and velocity. This volumetric field was then utilized as a (constant) background gas in the plasma simulations in order to model several reactions and interactions between the plasma and the neutral species without directly resolving all collisions with the Direct-simulation Monte-Carlo (DSMC) method.

1. Neutral gas

The neutral gas propellant was monoatomic xenon and an ionization efficiency of 5 % assumed.[10] Based on the mass flow of propellant during standard operation, and previous in-house simulations of the discharge chamber, a specific number density, temperature and axial inlet velocity could be determined at the vicinity of the screen grid inside the discharge chamber, serving as inlet conditions for the neutral gas simulation. The employed DSMC code was the open source software PICLas[11–13] and a fully-structured hexahedral mesh was devised with the criteria to locally resolve the mean free path and, on average, have no less than five particles per simulation cell. Further, an appropriate time step was chosen to ensure that the ratio between the time step and mean collision time in each cell remains below unity at all time. For collision modeling, the variable hard sphere (VHS) model by Bird[14] was used for Xe−Xe collisions. A reference kinetic diameter of 574 pm, viscosity coefficient of 0.85, temperature exponent of 273 K and reference velocity of 210 $\mathrm{m\,s^{-1}}$ were used.[15]

2. Plasma species

The plasma is simulated with the Particle-in-Cell (PIC) method and DSMC collisions are taken into account for each species binary collision combination. The electro-magnetic field is assumed stationary and a higher-order discontinuous Galerkin (HODG) Poisson solver is employed according to the governing equation

$$\nabla \cdot \mathbf{E} = \nabla^2 \phi = -\frac{\rho}{\epsilon}\,. \tag{1}$$

A fully-kinetic approach is utilized, tracking all charged species in space and time, as the Boltzmann relation assumption is not applicable for the investigated scenario with non-equilibrium regions. The plasma species consist of singly- and doubly charged xenon ions, and electrons. Each time step, all species are checked for collisions in each cell, including collisions with the neutral background gas, based on the collision probability that is determined from the kinetic energy and number density of the respective colliding species.

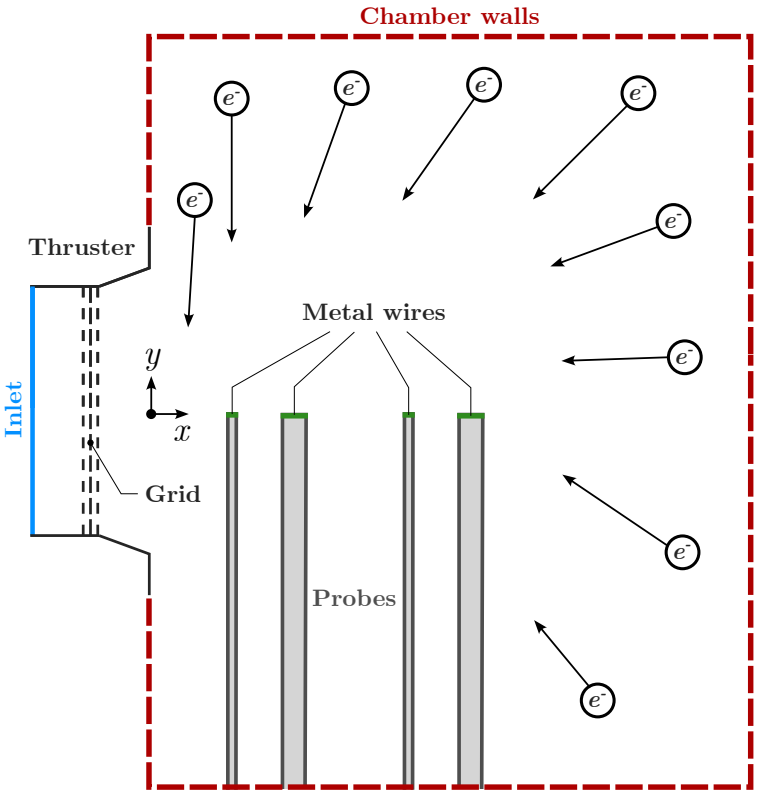

Figure 2. Schematic of numerical boundary conditions for the plasma simulations, highlighting the process of self-neutralization through SEE electrons attracted by the positive plasma potential of the exhaust plume.

Moreover, the colliding species are checked if certain reaction criteria are met. The considered reactions include

$$\mathrm{Xe} + \mathrm{e}^- \longrightarrow \mathrm{Xe}^+ + \mathrm{e}^- + \mathrm{e}^- \tag{2}$$

$$\mathrm{Xe} + \mathrm{Xe}^+ \longrightarrow \mathrm{Xe}^+ + \mathrm{Xe} \tag{3}$$

$$\mathrm{Xe}^+ + \mathrm{e}^- \longrightarrow \mathrm{Xe}^{++} + \mathrm{e}^- + \mathrm{e}^- \tag{4}$$

$$\mathrm{Xe} + \mathrm{Xe}^+ \longrightarrow \mathrm{Xe} + \mathrm{Xe}^{++} + \mathrm{e}^- \,. \tag{5}$$

Reaction-based chemistry is realized by means of cross-section databases provided by the software `LXCat`.[16] A schematic of numerical boundary conditions is shown in Fig. 2. Estimating the plasma potential at the inlet is realized by plasma sheath theory[12]

$$\phi_p = -\frac{k_B T_e}{e} \cdot \ln\left(u^{\mathrm{in}}_{\mathrm{Xe}^+} \sqrt{\frac{2\pi m_e}{k_B T_e}} \right) \,, \tag{6}$$

and the inlet velocity of electrons and ions is assumed to be 1.5× the Bohm velocity

$$u_{\mathrm{Bohm}} = \sqrt{\frac{k_B T_e}{m_{\mathrm{Xe}^+}}} \qquad \text{with } T_e \approx 5\,\mathrm{eV}\,. \tag{7}$$

Thus, at the inlet, fixed Dirichlet conditions are enforced for the potential, and plasma species properties. The potential of the each RIT grid is fixed according to the operating voltage, where $\phi_{\mathrm{decel}} = 0\,\mathrm{V}$. The boundary conditions of the probes are considered dielectrics, allowing charges to accumulate on the surface, while the measurement metal wires on top are allowed to float, based on the incoming flux of ions and electrons. At the outlet, a virtual SEE chamber is assumed, where in steady-state, the flux of impacting

ions equals the flux of emitted electrons. Hence, for each ion crossing the outlet, an electron is emitted with a random temperature according to a Maxwell-Boltzmann probability density distribution of $T_e = 3\,\mathrm{eV}$.

The mesh for the plasma simulations was iteratively devised in order to adequately resolve the Debye length of the electrons. The adjustment of the constant time step Δt underwent the same procedure, yielding $\Delta t = 5 \times 10^{-12}\,\mathrm{s}$, while a total number of fully-structured hexahedral cells of 1.5 million was devised.

III. Results and discussion

Experimental results of the measured radial-axis potential $\phi(y)$ are shown in Fig. 3 for various distances from the thruster exit plane. It is evident how the potential increases significantly from several volts up to few hundreds of volts as soon as the probes are located inside the exhaust plume. This finding is undermined by the fact that the blow-up extends further in radial distance for measurements taken at greater downstream distances due to the divergence of the ion beam.

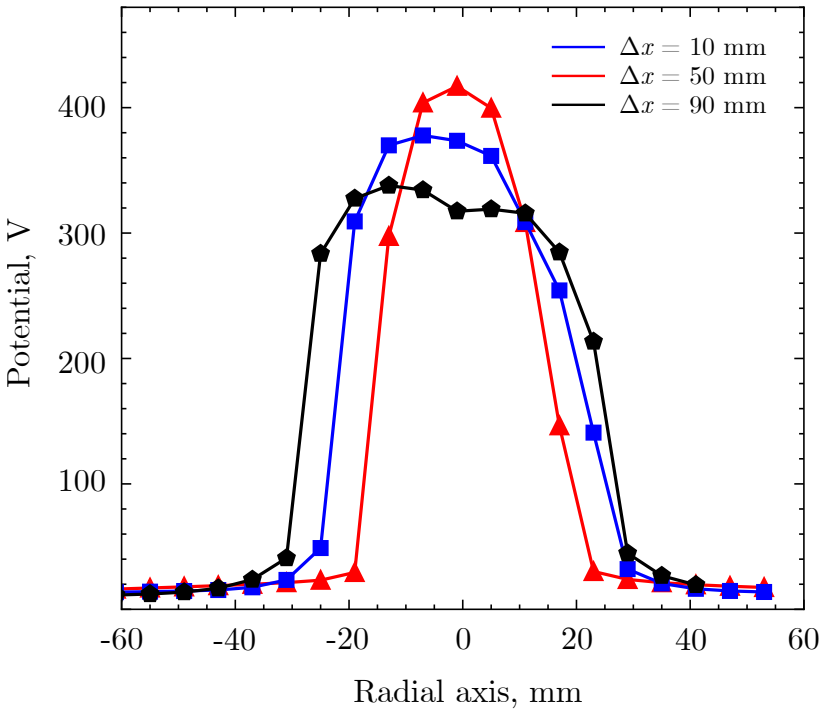

Figure 3. Radial probe measurement values of plasma potential during shift through exhaust plume. Clearly, an indication of potential blow-up is visible, reaching it's maximum at the centreline ($\Delta y = 0$).

The numerical results are illustrated in Fig. 4, showcasing the electron number density, xenon ion number density, xenon ion velocity, and plasma potential, respectively (row-by-row). The two columns delineate the two cases where no probes are located inside the beam (column 1) and the case where the probes are placed exactly at the centerline of the exhaust plume (column 2). In the disturbed case, the probe 1 was placed 10 mm downstream the thruster exhaust plane.

The electron number density in the first row indicates that the disturbed case results in the presence of more electrons in the probe area. In the second row, the xenon ion number density exhibits smooth contours and divergence and low beam divergence when no probes are present. However, the slowing down of ions close to the probes (row 3) suggests larger collision probabilities and the production of CEX ions in the probe region. Consequently, some random traces of radially escaping ions coupled with an increased beam divergence are found. The most severe difference is obtained for the plasma potential. In the undisturbed case, the values are in the range of a few volts, agreeing well with predictions made by plasma theory. Placing the probes inside the ion beam leads to a blow-up by several hundreds of volts, slowing down the ions and interfering with the SEE self-neutralization process by acting as a sink for fast moving electrons in bounded plasmas.

This circumstance is also reflected in Fig. 5, illustrating an axial centreline plot of the plasma potential

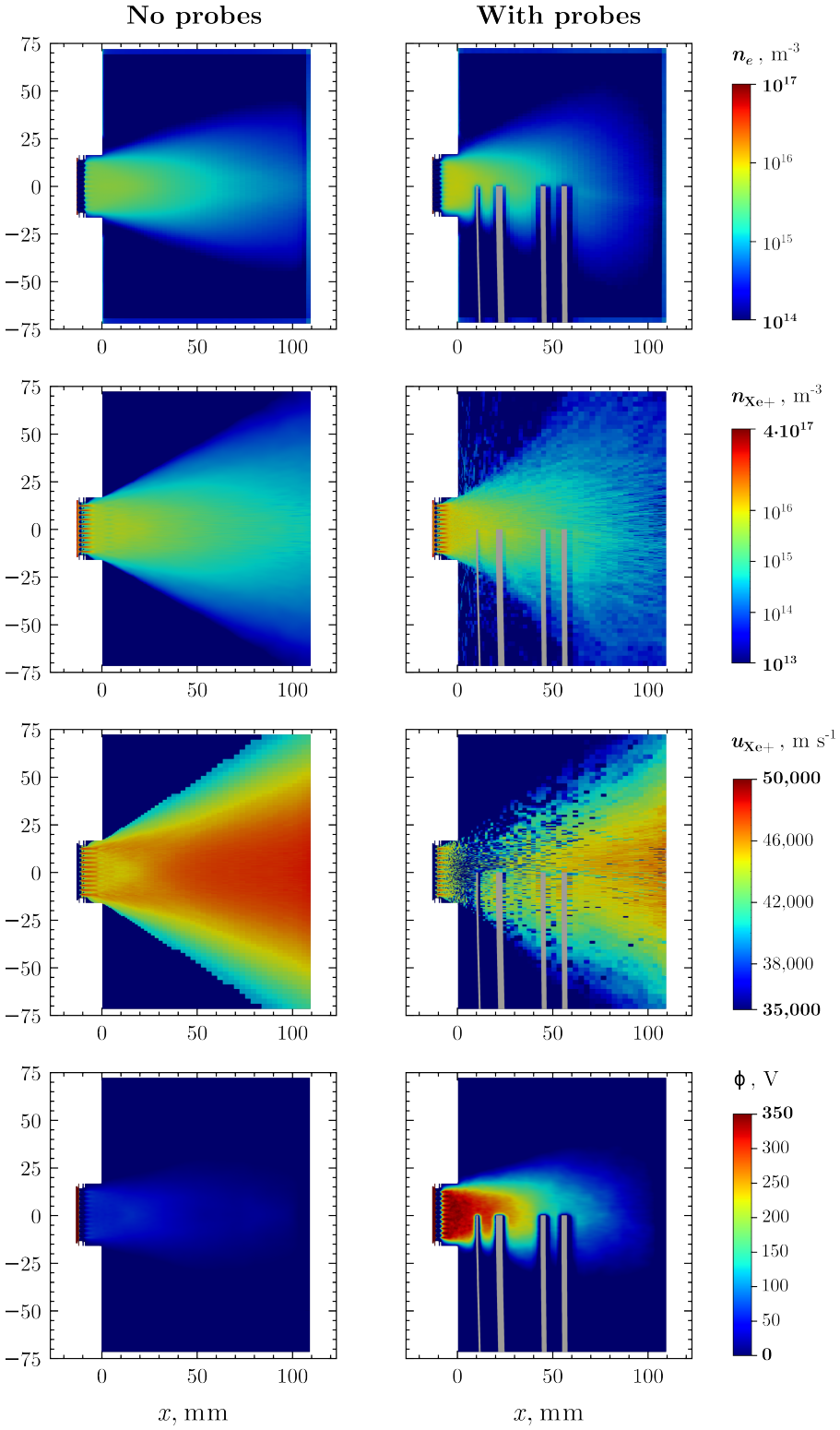

Figure 4. PIC-DSMC results for the fully *undisturbed* and fully *disturbed* cases, showing evidence of severe plasma disturbance by the presence of the probes inside the beam. Probes are place at a downstream distance of $\Delta x = 10$ mm. The left column indicates the undisturbed case, the right column the disturbed case. Row 1: Electron number density (log scale); row 2: ion number density (log scale); row 3: ion velocity; row 4: plasma potential.

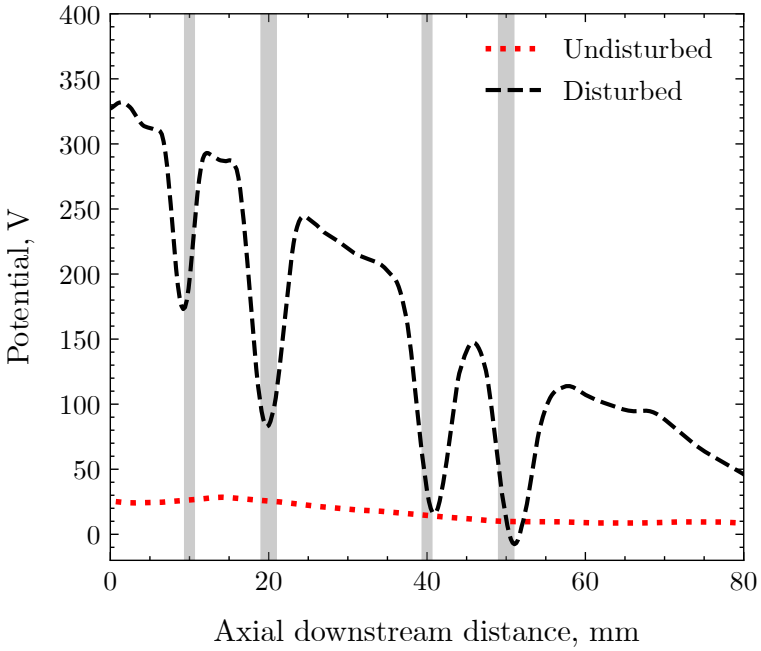

Figure 5. Axial centreline plot of plasma potential for the disturbed and undisturbed cases. Spatial probe placements are indicated by the grey areas.

$\phi(x)$ at $y, z = 0$. Clearly, the disturbed self-neutralization process results in up to 350 V of plasma potential according to the simulated case and is in good agreement with the values obtained in the experiment.

IV. Conclusion

An experimental and numerical study was performed in order to prove that the presence of probes located in the exhaust plume of EP thrusters (in our case a mN-RIT) exerts significant influence on the plasma properties when the process of space charge compensation relies on SEE through facility effects. Indeed, our study demonstrates an increase of the plasma potential by several hundreds of volts, proving the importance of exercising endurance or erosion tests *without* emissive probes, as the increased plasma potential would lead to much higher acceleration rates of CEX ions produced close to the thruster in the exhaust plume.

Acknowledgements

This work was financially supported by the European Space Agency [ESA contract number `4000129121-19-NL-RA`]. Computational resources (HPC-cluster HSUper) have been provided by the project `hpc.bw`, funded by `dtec.bw` – Digitalization and Technology Research Center of the Bundeswehr. `dtec.bw` is funded by the European Union – NextGenerationEU.

References

[1]Lobbia, R. B. and Beal, B. E., "Recommended practice for use of Langmuir probes in electric propulsion testing," *Journal of propulsion and power*, Vol. 33, No. 3, 2017, pp. 566–581. `http://dx.doi.org/10.2514/1.B35531`.

[2]Sheenan, J. P., Raitses, Y., Hershkowitz, N., and McDonald, M., "Recommended practice for use of emissive probes in electric propulsion testing," *Journal of propulsion and power*, Vol. 33, No. 3, 2017, pp. 614–637. `http://dx.doi.org/10.2514/1.B35697`.

[3]Kemp, R. F. and Sellen, J. M., J., "Plasma Potential Measurements by Electron Emissive Probes," *Review of Scientific Instruments*, Vol. 37, No. 4, 12 2004, pp. 455–461. `http://dx.doi.org/10.1063/1.1720213`.

[4]Smith, J. R., Hershkowitz, N., and Coakley, P., "Inflection-point method of interpreting emissive probe characteristics," *Review of Scientific Instruments*, Vol. 50, No. 2, 08 2008, pp. 210–218. `http://dx.doi.org/10.1063/1.1135789`.

[5]Li, P., Hershkowitz, N., Wackerbarth, E., and Severn, G., "Experimental studies of the difference between plasma

potentials measured by Langmuir probes and emissive probes in presheaths," *Plasma sources science and technologie*, Vol. 29, 2020. http://dx.doi.org/10.1088/1361-6595/ab69e5.

[6]Riege, H., "Neutralization principles for the extraction and transport of ion beams," *Nuclear Instruments and Methods in Physics Research Section A: Accelerators, Spectrometers, Detectors and Associated Equipment*, Vol. 451, No. 2, 2000, pp. 394–405. http://dx.doi.org/10.1016/S0168-9002(00)00322-3.

[7]Wirz, R. E., Anderson, J., Goebel, D. M., and Katz, I., "Decel Grid Effects on Ion Thruster Grid Erosion," *IEEE Transactions on Plasma Science*, Vol. 36, 2008, pp. 2122–2129.

[8]Feili, D., Smirnova, M., Dobkevicius, M., Perez, A. M., Lotz, B., and Collingwood, C., "Design, construction and testing of a radio frequency mini ion engine according to the propulsion requirements of the next generation gravity mission 'NGGM'," No. 34 in International Electric Propulsion Conference, Hyogo-Kobe, Japan, 2015, p. 277.

[9]Kozakov, R., Maigler, M., Schein, J., and Wallace, N., "Determination of Self-Neutralization Phenomena of Ion Beams with Langmuir Probe Measurements and PIC-DSMC Simulations," *Applied Sciences*, Vol. 14, No. 8, 2024. http://dx.doi.org/10.3390/app14083470.

[10]Dobkevicius, M., *Modelling and design of inductively coupled radio frequency gridded ion thrusters with an application to Ion Beam Shepherd type space missions*, Ph.D. thesis, University of Southampton, 2017.

[11]Ortwein, P., Copplestone, S., Munz, C.-D., Binder, T., Mirza, A., Nizenkov, P., Pfeiffer, M., Reschke, W., and Fasoulas, S., "Piclas: A Highly Flexible Particle Code for the Simulation of Reactive Plasma Flows," *2017 IEEE International Conference on Plasma Science (ICOPS)*, 2017. http://dx.doi.org/10.1109/plasma.2017.8496309.

[12]Binder, T., *Development and application of PICLas for combined optic-/plume-simulation of ion-propulsion systems*, Phd thesis, University of Stuttgart, 2019. http://dx.doi.org/10.18419/opus-10657.

[13]Pfeiffer, M., Hindenlang, F., Binder, T., Copplestone, S., Munz, C.-D., and Fasoulas, S., "A particle-in-cell solver based on a high-order hybridizable discontinuous Galerkin spectral element method on unstructured curved meshes," *Computer Methods in Applied Mechanics and Engineering*, Vol. 349, 2019, pp. 149–166.

[14]Bird, G. A., *The DSMC Method: Version 1.2, 2013*, CreateSpace, 2013.

[15]Bird, G., *Molecular Gas Dynamics and the Direct Simulation of Gas Flows*, Clarendon Press, Oxford, 1994.

[16]Pitchford, L. C., Alves, L. L., Bartschat, K., Biagi, S. F., Bordage, M.-C., Bray, I., Brion, C. E., Brunger, M. J., Campbell, L., Chachereau, A., Chaudhury, B., Christophorou, L. G., Carbone, E., Dyatko, N. A., Franck, C. M., Fursa, D. V., Gangwar, R. K., Guerra, V., Haefliger, P., Hagelaar, G. J. M., Hoesl, A., Itikawa, Y., Kochetov, I. V., McEachran, R. P., Morgan, W. L., Napartovich, A. P., Puech, V., Rabie, M., Sharma, L., Srivastava, R., Stauffer, A. D., Tennyson, J., de Urquijo, J., van Dijk, J., Viehland, L. A., Zammit, M. C., Zatsarinny, O., and Pancheshnyi, S., "LXCat: an Open-Access, Web-Based Platform for Data Needed for Modeling Low Temperature Plasmas," *Plasma Processes and Polymers*, Vol. 14, No. 2, 2017. http://dx.doi.org/10.1002/ppap.201600098.